

Washington University School of Medicine

**Digital Commons@Becker**

---

2020-Current year OA Pubs

Open Access Publications

---

7-1-2022

**Motor network reorganization induced in chronic stroke patients with the use of a contralesionally-controlled brain computer interface**

Joseph B. Humphries

Daniela J S Mattos

Jerrel Rutlin

Andy G S Daniel

Kathleen Rybczynski

*See next page for additional authors*

Follow this and additional works at: [https://digitalcommons.wustl.edu/oa\\_4](https://digitalcommons.wustl.edu/oa_4)

---

---

**Authors**

Joseph B. Humphries, Daniela J S Mattos, Jerrel Rutlin, Andy G S Daniel, Kathleen Rybczynski, Theresa Notestine, Joshua S. Shimony, Harold Burton, Alexandre Carter, and Eric C. Leuthardt



## Motor Network Reorganization Induced in Chronic Stroke Patients with the Use of a Contralesionally-Controlled Brain Computer Interface

Joseph B. Humphries, Daniela J. S. Mattos, Jerrel Rutlin, Andy G. S. Daniel, Kathleen Rybczynski, Theresa Notestine, Joshua S. Shimony, Harold Burton, Alexandre Carter & Eric C. Leuthardt

To cite this article: Joseph B. Humphries, Daniela J. S. Mattos, Jerrel Rutlin, Andy G. S. Daniel, Kathleen Rybczynski, Theresa Notestine, Joshua S. Shimony, Harold Burton, Alexandre Carter & Eric C. Leuthardt (2022) Motor Network Reorganization Induced in Chronic Stroke Patients with the Use of a Contralesionally-Controlled Brain Computer Interface, *Brain-Computer Interfaces*, 9:3, 179-192, DOI: [10.1080/2326263X.2022.2057757](https://doi.org/10.1080/2326263X.2022.2057757)

To link to this article: <https://doi.org/10.1080/2326263X.2022.2057757>



© 2022 The Author(s). Published by Informa UK Limited, trading as Taylor & Francis Group.



[View supplementary material](#)



Published online: 01 Jul 2022.



[Submit your article to this journal](#)



Article views: 919



[View related articles](#)



[View Crossmark data](#)



Citing articles: 1 [View citing articles](#)

# Motor Network Reorganization Induced in Chronic Stroke Patients with the Use of a Contralesionally-Controlled Brain Computer Interface

Joseph B. Humphries<sup>a</sup>, Daniela J. S. Mattos<sup>b</sup>, Jerrel Rutlin<sup>c</sup>, Andy G. S. Daniel<sup>a</sup>, Kathleen Rybczynski<sup>d</sup>, Theresa Notestine<sup>d</sup>, Joshua S. Shimony<sup>e</sup>, Harold Burton<sup>e</sup>, Alexandre Carter<sup>b</sup> and Eric C. Leuthardt<sup>a,d,e,f\*</sup>

<sup>a</sup>Departments of Neurosurgery, Washington University in St. Louis, St. Louis, MO, USA; <sup>b</sup>Neurology, Washington University in St. Louis, St. Louis, MO, USA; <sup>c</sup>Mallinckrodt Institute of Radiology, Washington University in St. Louis, St. Louis, MO, USA; <sup>d</sup>Neurosurgery, Washington University in St. Louis, St. Louis, MO, USA; <sup>e</sup>Neuroscience, Washington University in St. Louis, St. Louis, MO, USA; <sup>f</sup>Mechanical Engineering and Materials Science, Washington University in St. Louis, St. Louis, MO, USA

## ABSTRACT

Upper extremity weakness in chronic stroke remains a problem not fully addressed by current therapies. Brain–computer interfaces (BCIs) engaging the unaffected hemisphere are a promising therapy that are entering clinical application, but the mechanism underlying recovery is not well understood. We used resting state functional MRI to assess the impact a contralesionally driven EEG BCI therapy had on motor system functional organization. Patients used a therapeutic BCI for 12 weeks at home. We acquired resting-state fMRI scans and motor function data before and after the therapy period. Changes in functional connectivity (FC) strength between motor network regions of interest (ROIs) and the topographic extent of FC to specific ROIs were analyzed. Most patients achieved clinically significant improvement. Motor FC strength and topographic extent decreased following BCI therapy. Motor recovery correlated with reductions in motor FC strength across the entire motor network. These findings suggest BCI-mediated interventions may reverse pathologic strengthening of dysfunctional network interactions.

## ARTICLE HISTORY

Received 12 July 2021  
Accepted 20 March 2022

## KEYWORDS



Rehabilitation; stroke; brain–computer interface; functional MRI; motor network

## 1. Introduction


Stroke causes adult disability in approximately 800,000 adults annually in the United States [1]. Unilateral upper motor weakness, known as hemiparesis, occurs in 77% of new stroke cases [2]. Hemiparesis frequently persists into the chronic stage of stroke; 65% of chronic stroke patients report reduced motor function 6 months after stroke [3,4]. Patients rarely obtain substantial motor improvement 3 months after a stroke, with residual motor deficits effectively becoming permanent [5–11]. Behavioral adaptations instead of spontaneous recovery generally underlie subsequent improvements [9]. Recent innovations in rehabilitation techniques, however, offer new opportunities for motor recovery, even in the chronic stage.

The efficacy of brain–computer interfaces (BCIs) for post-stroke motor rehabilitation has been demonstrated with a variety of designs [12]. However, there is a lack of consensus regarding the neurophysiological mechanisms driving recovery through BCI [13–16], which necessitated further study. Functional recovery was previously shown in a severely impaired chronic stroke

population treated with a BCI system using signals from the contralesional motor cortex [17]. The former study used cortical EEG signals to control a robotic hand orthosis. Additionally, the efficacy of BCI on motor recovery was linked to changes in EEG activity in motor regions within frequencies used for BCI [17]. Given that this contralesional BCI system, known as the IpsiHand (Neuroolutions, Santa Cruz CA), recently received FDA market authorization and will be applied to stroke populations, understanding the mechanism of its clinical benefit is of high importance. Power fluctuations in alpha (8–12 Hz) and beta (13–25 Hz) frequencies are observed in motor cortex during motor activity [18,19]. These frequencies are also used for BCI control [17]. We therefore hypothesized BCI may have affected neural circuitry to facilitate motor recovery via experience-dependent plasticity. However, previously recorded EEG signals only assess broad cortical regions with limited anatomic specificity. Here, we used functional MR imaging to study whether BCI therapy affected functional connectivity organization in the motor cortex and cerebellum.

**CONTACT** Eric C. Leuthardt  [leuthardt@wustl.edu](mailto:leuthardt@wustl.edu)  Department of Neurological Surgery, Washington University in St. Louis, 660 S. Euclid Avenue, Campus Box 807, St. Louis, MO 63110, USA

\*Drs. Carter and Leuthardt contributed equally to this project.

 Supplemental data for this article can be accessed online at <https://doi.org/10.1080/2326263X.2022.2057757>

© 2022 The Author(s). Published by Informa UK Limited, trading as Taylor & Francis Group.

This is an Open Access article distributed under the terms of the Creative Commons Attribution-NonCommercial-NoDerivatives License (<http://creativecommons.org/licenses/by-nc-nd/4.0/>), which permits non-commercial re-use, distribution, and reproduction in any medium, provided the original work is properly cited, and is not altered, transformed, or built upon in any way.

Networks of correlated spontaneous brain activity during rest have been extensively described using functional MRI (fMRI) [20–22]. Strokes disrupt ‘functional connectivity’ networks [23–26]. Furthermore, the extent of network disruption correlated with stroke-induced impairments in multiple behavioral domains [23,25–27]. Strokes altered network modularity, typically by a decrease and then a partial recovery in association with behavioral improvements [25,28,29]. Connectivity changes between specific regions have also been implicated in stroke recovery [30–32]. Further, performance on motor function assessment tasks after a stroke was reduced with disrupted interhemispheric motor network connectivity [24,33]. Thus, recovery from stroke induced by BCI might involve changes in resting-state functional connectivity (rsFC).

The objective of the current study was to determine whether an EEG-driven BCI controlled by motor signals from the unaffected hemisphere reorganized brain networks for motor control. Based on previous reports linking motor network organization with post-stroke motor function, we hypothesized that motor recovery achieved during BCI therapy would change motor network connectivity, and that these rsFC changes in motor systems would correlate with the strength of recovery. Increases in interhemispheric connectivity, and decreases in intrahemispheric connectivity have previously been reported during stroke recovery [24,25,30,33–35]. Consequently, we hypothesized motor recovery via BCI would lead to similar patterns of change in inter- and intrahemispheric rsFC. The unexpected findings in this study suggest a potential novel recovery mechanism associated with BCI induced recovery in chronic stroke.

## 2. Materials and methods

### 2.1. Patient demographics

Eight enrolled patients had an upper limb hemiparesis (Median upper extremity portion of the Fugl-Meyer Assessment (UEFM) = 21.75) at least 6 months

post-stroke. Exclusion criteria included evidence of memory loss, severe aphasia, joint contractures in the upper limb, unilateral neglect, or an inability to generate a consistent BCI control signal. A complete list of inclusion and exclusion criteria is available in the supplemental material. Table 1 details patient demographic information. Most patients showed a moderate or severe motor impairment, although two patients showed a mild impairment. Every patient provided written informed consent before data collection.

### 2.2. EEG screening

Patients performed an EEG screening task to identify a brain signal associated with motor imagery of the affected hand from the contralesional hemisphere (i.e. the BCI control feature). Patients had to generate the motor imagery EEG signal consistently for the BCI therapy task. Initially, patients rested quietly for approximately 7 minutes during recordings of baseline EEG activity. Patients then performed a series of paired trials of quiet rest and imagined movement of their left, right, or both hands at the same time. Trial duration was 8 seconds with an inter-trial interval of 3 seconds. A single EEG screening session included acquisition of approximately 45 trials of rest and each type of imagined hand motion. Patients had to avoid moving or talking during EEG recordings. Screenings paused automatically for patients to rest in absence of a specific task at 25% completion intervals for the full duration of the screening. Each patient performed at least two screening sessions. A third session was necessary when detected feature frequencies were erratic or EEG signal quality was low in a prior session. Excluded patients had low-quality EEG data in all screening sessions, showed no reliable feature frequency, or could not regularly perform the BCI task.

**Table 1.** Demographic information.

Patient ID	Age (y)	Time Post-Stroke (mo.)	Gender	Lesion Location	Affected Limb	UEFM Baseline	UEFM Final	UEFM Change
1	55	183	F	L SMC	R	56	64	8
2	55	54	F	L BG, Thal	R	41	48	7
3	60	119	M	R BG, CST, L Thal	L	25.5	30	4.5
4	56	34	M	L BG, CST	R	19.5	25	5.5
5	68	46	M	L BG, Thal, CST	R	14.5	22	7.5
6	74	26	F	R BG, CST	L	12	21	9
7	63	71	M	L BG, CST, R BG	R	21.5	32	10.5
8	38	70	M	R BG, Thal, CST	L	22	31	9
Median	58	62				21.75	30.5	7.75

SMC: Somatomotor Cortex, BG: Basal Ganglia, Thal: Thalamus, CST: Corticospinal Tract.

### 2.3. BCI feature frequency

Control of the BCI device was through a 1 Hz wide feature frequency distinctly identified from EEG screening data in each patient. Stroke disrupts normal cortical oscillations in sensorimotor frequencies [36,37]. A patient-specific feature frequency approach was therefore implemented to lessen the impact of stroke-induced changes in the sensorimotor rhythm, which is classically used to control motor BCIs. The band-limited power of the feature frequency determined whether the orthosis opened (decreased power) or closed (increased power) during BCI therapy. A detailed description of BCI control signal processing is available in the supplemental material. A measure of the variance in each feature frequency from each patient was its coefficient of determination ( $R^2$ ), calculated from the difference in quiet rest and impaired hand imagery task states in each screening session. Negative  $R^2$  values indicated a power decrease during motor imagery relative to rest. Selected from each patient were feature frequencies with the largest negative  $R^2$  value within mu or beta frequency bands (8–25 Hz) dependably produced across screening sessions.

### 2.4. Intervention protocol

The study timeline started with screening sessions over 1–2 weeks, followed by pre-therapy motor assessments and resting-state fMRI (Figure 1(a)). Next, patients trained to use the BCI device. They subsequently received a complete set of equipment to use at home. Patients then performed 12 weeks of home BCI therapy sessions, when they used the equipment for 1 hour per day, 5 days per week. The assigned therapy sessions totaled 60 hours. Although all patients were assigned the same amount of BCI therapy, usage varied among patients. Therapy dosage for BCI patients was estimated by summing the number of runs with at least 10% accuracy on both movement imagery and rest trials. Five BCI runs were approximately one hour of therapy. Patients either performed the therapy and device setup alone or with a caretaker based on their specific needs and living situation. Members of the research team were available via phone and e-mail to assist with technical issues. Excluded from the study were patients unable to use the BCI device. Patients had to enter their usage on a provided tracking sheet, which assisted them in documenting therapy times and any problems experienced with the equipment. Clinicians assessed motor function

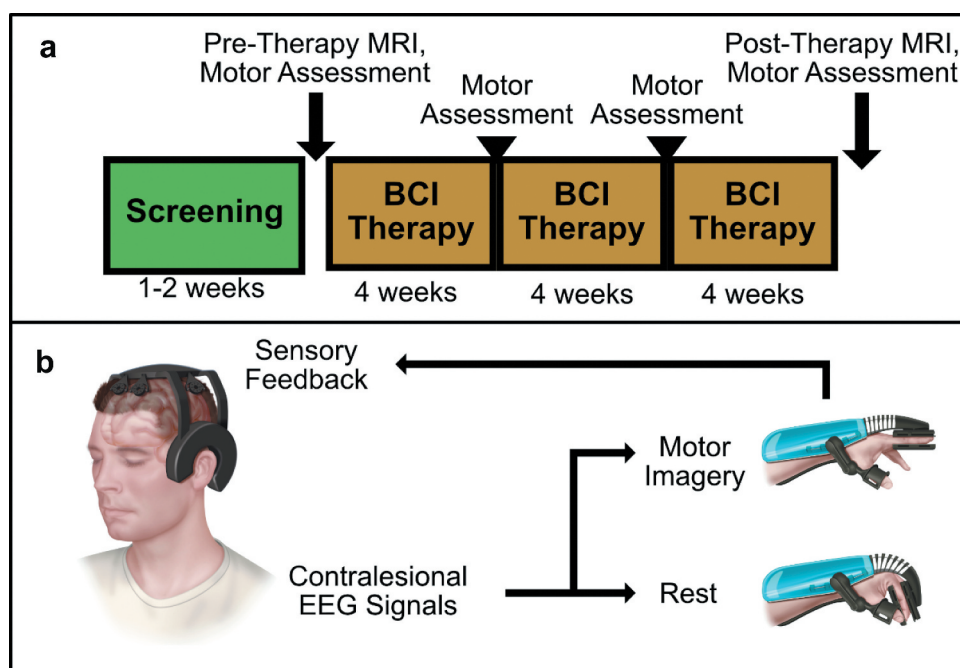


**Figure 1.** BCI Intervention protocol and system design overview. (a) Protocol Timeline. Screening for EEG feature frequency and inclusion and exclusion criteria occur over several sessions in a 1–2 week period. Following screening, patients undergo an MRI scan and motor assessments before receiving their BCI device. Patients perform BCI therapy for 12 weeks at home, returning every 4 weeks for motor assessments. A final MRI scan and motor assessment is performed after 12 weeks of therapy. (b) BCI System Design.

once per month (Figure 1(a)). After 12 weeks of BCI therapy, patients received a post-therapy motor assessment and second resting-state fMRI scan. Patients in the comparison group received intensive physical therapy in an 8-week task-specific training program.

## 2.5. BCI system design

Components of the BCI system included a motorized hand orthosis and wireless EEG headset (Wearable Sensing, San Diego, CA) with dry, active electrodes (Figure 1(b)). A Windows tablet connected via bluetooth to the EEG headset to record signals from the electrodes. A local Wi-Fi network generated within the orthosis supported communications between the tablet and a computer within the orthosis. The computer controlling orthosis received commands to open or close the hand via the tablet through these communications.

BCI therapy sessions involved multiple steps: (1) Patients put on the BCI headset and hand orthosis, turned on system components, and confirmed correct communications through a series of automated test outputs. The index and middle fingers of the affected limb were placed into padded braces where they could be flexed and extended with the orthosis. The motor and electronics in the orthosis were contained inside the device and rested on the forearm of the affected limb. After powering on the system components, the BCI control software loaded onto the tablet checked for connections to the headset and orthosis. Upon confirmation of these connections, the software proceeded to signal quality assessment. (2) Next, EEG signal quality assessments involved comparing low amplitude rest signals to noisy signals activated by jaw clenches. Patients were prompted to rest and clench their jaws, each for 5 seconds. Raw signals were displayed to the patients during this process, and they were trained to identify the characteristic noise expected during clenching. Following the rest and clench states, an electrode map was displayed with colors (green, yellow, and red) denoting signal quality at each electrode site. Quality was assessed by measuring the difference in signal power between rest and clench states, as a jaw clench typically results in significantly higher signal power. When signals were too noisy, patients could improve electrode connections by manually adjusting the headset and electrodes to facilitate contact with the scalp, rotating electrodes to push through hair, and waiting for a gradual decline in dry electrode impedance. Therapy did not proceed until signal quality improved with a subsequent assessment. (3) Patients began the BCI therapy task following a one-minute recording of an at-

rest signal and eight repetitions each of 8-second-long quiet rest and motor imagery trials. These recordings enabled threshold adjustments for orthosis control for each session. During therapy, patients received a cue to remain quietly at rest or perform vivid motor imagery of their affected hand. Band-limited power of the feature frequency was extracted from the contralesional EEG signal during therapy. The hand orthosis opened in a 3-point grip (Figure 1(b), upper right) after power of the feature frequency dropped below the threshold. The orthosis remained closed at higher feature frequency power levels (Figure 1(b), lower right). Patients received an instruction to attempt opening the orthosis by thinking about moving during motor imagery trials, and kept the hand closed by clearing their thoughts during rest trials. Patients thereby received proprioceptive and visual sensory feedback from the orthosis based on the EEG signals they generated. Individual trials lasted 8 seconds followed by a 3-second inter-trial interval.

## 2.6. Motor function assessment

The upper extremity portion of the Fugl-Meyer Assessment functioned as the primary motor outcome due to its wide use and high inter- and intra-rater reliability [38–40]. UEFM is a 66-point measurement of reaching and grasping ability with several hand orientations and ranges of motion. Secondary outcomes included grip strength, Motricity Index, Modified Ashworth Scale (MAS), and Arm Motor Ability Test (AMAT) [41–43]. Motor function assessment to establish a stable baseline occurred twice before commencing therapy. Baseline motor function was the average of two assessments ( $pre_1$  and  $pre_2$ ). Further assessments occurred at 4-week intervals during therapy, and at 6-months post-therapy completion. Calculation of motor improvement followed the formula:

$$UEFM_{post} - \frac{UEFM_{pre1} + UEFM_{pre2}}{2},$$

that is, the post-therapy motor function score minus the average of the baseline motor function scores. Occupational and physical therapists assessed motor function.

## 2.7. MRI acquisition protocol

MRI scans with a Siemens Prisma 3 T scanner included structural images from T1-weighted MP-RAGE, T2-weighted fast spin echo, and fluid attenuation inversion recovery (FLAIR) sequences. Scanning sessions occurred within 2 weeks of initiating and completing



the 12-week therapy protocol. Capture of BOLD signals for resting-state data utilized a 64-channel head coil and a gradient echo EPI sequence (voxel size =  $2.4 \times 2.4 \times 2.4$  mm; TR = 1070 ms; TE = 30 ms; flip angle =  $70^\circ$ ; multi-band factor 4). Each of three, approximately 7-minute scans collected 400 frames of resting-state functional MRI data, for a total of 1200 frames over 21 minutes. We acquired distortion maps immediately prior to each resting-state BOLD scan.

Comparison group MRI scans included similar T1- and T2-weighted structural images with a Siemens TRIO 3 T scanner. Resting state BOLD data acquisition included the following parameters: 4 mm isotropic voxels; TR = 2000 ms; TE = 27 ms; 12 channel head coil; 4 scans with 128 frames each.

## 2.8. MRI preprocessing

A previously described pipeline preprocessed all functional MRI data [44]. The 4dfp suite (4dfp.readthedocs.io) of preprocessing steps comprised slice-time correction, removal of odd-even slice intensity differences, rigid body motion correction, affine transformation to a  $(3 \text{ mm})^3$  atlas space, spatial smoothing with a 6 mm FWHM Gaussian kernel, voxelwise linear detrending, and a temporal low pass filter (0.1 Hz cutoff). Freesurfer software performed cortical surface segmentation. Regression of nuisance waveforms, derived from motion correction timeseries, CSF signal, white matter signal, and the whole brain ('global') signal, reduced spurious variance [45,46]. High-motion frames were removed from the analysis [44]. Fisher z-transforms were applied to Pearson correlation coefficients prior to statistical analysis.

## 2.9. Seed-based functional connectivity calculations

Analysis of preprocessed MRI data utilized MATLAB (MathWorks, Natick, MA) unless otherwise noted. Cortical regions previously implicated in motor control served as *a priori* regions of interest (ROIs). These included the hand region of bilateral primary dorsal motor cortex (M1), dorsal premotor area (PMA), and supplementary motor area (SMA). We used Neurosynth [47] for all cortical ROI coordinates. Peak Z-scores for each ROI served as centers for 8 mm diameter spheres. Extracted mean BOLD timeseries were from each ROI. Generation of two aggregate cerebellum (CBL) ROIs were from somatomotor regions in anterior CBL lobules. Separately averaged left and right CBL somatomotor regions formed the

basis of left and right CBL mean timeseries [48]. Then, labeling these left- and right-side timeseries as contralesional and ipsilesional was relative to the left/right stroke brain location. Cerebellar laterality was in correspondence to motor network membership (i.e. left cerebellum and right primary motor cortex were in the same functional hemisphere). Excluded ROIs overlaid the stroke lesion. Analyses were of functional connectivity, defined as the Pearson correlation of paired mean ROI timeseries and between select ROIs and all other voxels in the brain. Pre- and post-therapy connectivity differences indicated changes in functional connectivity.

## 2.10. Functional connectivity analyses

A twofold focus of the functional connectivity analysis was: 1) define changes in cortical and subcortical connectivity topography and 2) define alterations in magnitude of connectivity in known motor network ROIs. For network topography, primary analyses performed on fMRI data included voxel-based functional connectivity between ROI in contralesional M1, ipsilesional M1, contralesional CBL, and ipsilesional CBL and the rest of the brain. Findings assessed connectivity changes at specific ROIs following BCI therapy. We examined only statistically significant functional connectivity maps by applying a threshold of  $z = 0.3$ . Obtained maps were from pre- and post-therapy timepoints. Counts of suprathreshold voxels in each connectivity map tracked spatial distributions for pre- and post-therapy MRI scans. Voxel counts were from the whole brain and each hemisphere. Wilcoxon signed-rank tests compared pre- and post-therapy timepoints for whole-brain voxel counts. Timepoints here refers to MRI scans at baseline before any therapy (pre-therapy) and after 12 weeks of BCI therapy (post-therapy). Suprathreshold voxel counts for each patient and ROI evaluated relationships between functional topography plasticity and motor recovery. The subtraction of pre- from post-therapy voxel counts quantified changes. Spearman rank correlations estimated the relationship between motor recovery and change in number of suprathreshold voxels.

Evaluations of motor network connectivity changes following therapy relied on assessments of network strength through pairwise functional connectivity (FC) measurements between ROIs. Median adjacency matrices generated from Pearson correlation coefficients between each ROI pair visualized FC



strength in the pre-therapy state as well as changes in FC following therapy. Adjacency matrices were converted into circular graphs for visualization using the Python NetworkX package [49]. Circular graph nodes were per ROI. Color of edges (lines) connecting nodes mark the z-score value of Pearson correlations (i.e. connectivity strength).

Pairwise connectivity measurements were grouped into the following subsets: all motor ROI pairs, inter-hemispheric ROI pairs contralesional intrahemispheric pairs, and ipsilesional intrahemispheric pairs. Interhemispheric ROI pairs indicated FC strengths between contra- and ipsilesional ROIs. For each ROI pair within these groupings, FC strengths across all cases were combined into distributions showing the proportion of each FC strength value at pre- and post-therapy timepoints. Similarly, distributions of all FC z-values for each ROI pair and per patient showed individual differences in changed FC strengths between pre- and post BCI therapy. Wilcoxon signed-rank tests assessed differences between pre- and post-therapy FC strength distributions relative to the number of correlation z-scores of a given magnitude. The formula listed below estimated the Wilcoxon signed-rank effect sizes:

$$r = Z/\sqrt{N},$$

with  $r$  the effect size,  $Z$  the signed-rank test Z-statistic, and  $N$  the sample size. The Spearman rank correlation between Wilcoxon effect sizes and increases in UEFM scores examined the relationships between FC change and motor recovery.

### 3. Results

#### 3.1. Motor rehabilitation

All BCI patients showed an increase in UEFM score after 12 weeks of contralesional BCI therapy. Clinically meaningful recovery occurred in seven of the eight patients who reached a minimal clinically important difference (MCID) threshold of at least a 5.2 point score increase [50]. Median increase in UEFM score was 7.25. Figure 2 illustrates progressive longitudinal motor recovery from baseline in each case. Most patients passed the clinically significant threshold by 8 weeks. Patients 1 and 2 showed similar UEFM improvement to other subjects despite having a much milder baseline impairment. Wilcoxon signed-rank tests also found significant improvement ( $p < 0.05$ ) in grip strength, Motricity Index score, and AMAT scores (see Supplemental Material for more detail). Median changes included increased grip strength (3.75 pounds,  $p = 0.0234$ ), Motricity Index (2 points,  $p = 0.0156$ ), and AMAT (5 points,  $p = 0.0156$ ). The Modified Ashworth Scale, a measure of spasticity, showed median changes of 0 at the elbow and 0.125 at the wrist. No MCID comparisons were available for these measures. Individual changes in secondary outcomes are detailed in Table S1.

#### 3.2. BCI performance

Patients generally used their BCI systems effectively, achieving median move and rest success rates of 78.5% and 35%, respectively. A definition of

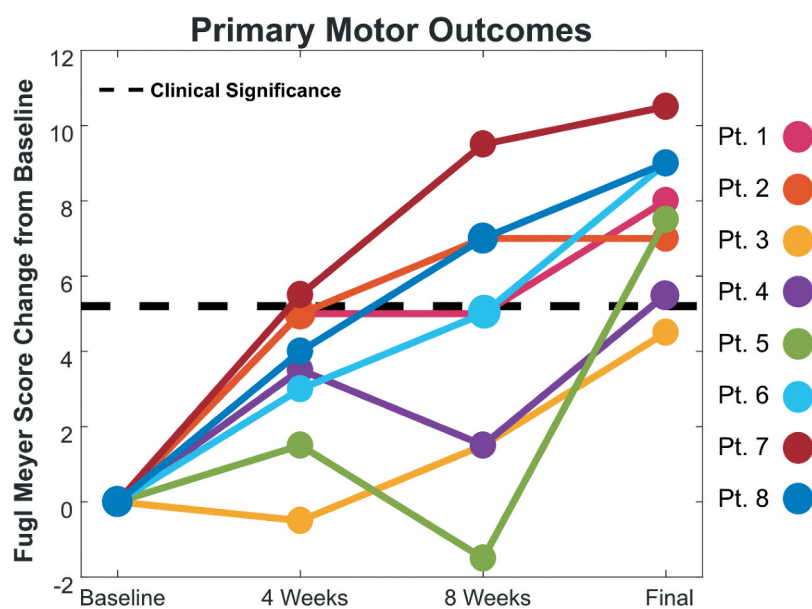


**Figure 2.** Longitudinal BCI primary motor outcomes. Longitudinal change in UEFM score from baseline. Each patient represented as a different line color. Dotted black line indicates minimal clinically important difference of 5.2 points on the UEFM.

**Table 2.** BCI performance data.

Subject	Move Success Rate (%)	Rest Success Rate (%)	Move Error (SS)	Rest Error (SS)	$R^2$	Total Sessions	Total Trials	Feature Frequency (Hz)
1	84	15	3.7	2.7	0.089	47	6120	21
2	49	48	3.9	4.1	0.102	62	9660	15
3	34	60	2.8	2.8	0.089	19	2790	19
4	92	23	3.6	3.8	0.256	50	8250	15
5	73	37	3.1	3.2	0.239	61	9750	16
6	31	62	4.7	4.9	0.128	29	3690	11
7	96	33	18.5	4.1	4.145	86	9420	10
8	91	22	18.5	3.3	3.341	26	3090	18

SS: Sum of Squares,  $R^2$ : Coefficient of Determination, Bold denotes updated hardware algorithm which changes estimation of error and  $R^2$ .

a successful trial was reaching the BCI activation threshold for at least 1 second for move trials or staying under the activation threshold for the entire trial duration for rest trials. Most patients showed greater success rates with movement imagery trials due to restrictive criteria for success on rest trials. Although we accepted feature frequencies in both alpha (8–12 Hz) and beta (13–25 Hz) bands, six out of eight patients had beta feature frequencies. This preference for beta frequencies is consistent with previous studies of ipsilateral motor electrophysiology in which there are stronger spectral power changes in the beta band than in the mu (also known as alpha) band during ipsilateral movement [51].

Table 2 contains BCI performance data including feature frequencies, trial success rates, signal error (Sum of Squares), and coefficients of determination ( $R^2$ ).

### 3.3. Spatial distributions of voxel-based functional connectivity in select ROIs

BCI therapy-induced changes in spatial connectivity patterns in contralesional and ipsilesional primary motor cortex and cerebellum from pre- and post-therapy in group average functional connectivity maps ( $z > 0.3$ ), as shown in Figure 3. Qualitatively, contralesional and ipsilesional M1 (Figure 3(a,b)) and cerebellar

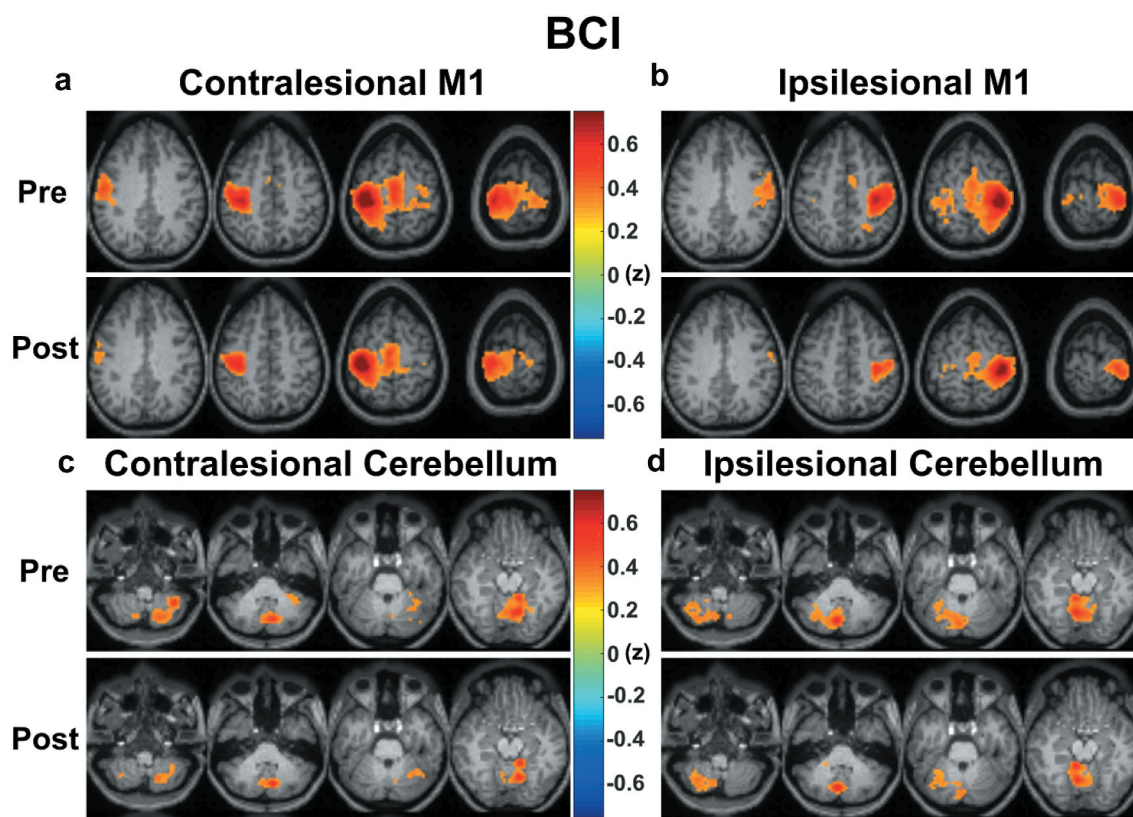


**Figure 3.** Spatial connectivity distributions change following BCI Therapy. Pre- and post-therapy maps of group average voxelwise functional connectivity ( $z > 0.3$ ) are shown for contralesional M1 (a), ipsilesional M1 (b), contralesional cerebellum (c), and ipsilesional cerebellum (d). Pre-therapy maps are shown above their post-therapy equivalents.

(Figure 3(c,d)) ROIs showed decreased spatial distributions functional connectivity voxels post therapy (Figure 3(a–d)). Smaller extents of functional connectivity appeared especially in ipsilesional M1 (Figure 3(b)) and contralesional cerebellum (Figure 3(c)).

Quantitatively, suprathreshold voxel counts significantly decreased for ipsilesional M1 following BCI therapy (Figure 4, Wilcoxon signed-rank test,  $p = 0.0156$ ). Suprathreshold voxel count changes were normalized to the matching baseline for each patient and region. Box-and-whisker plots of pre- and post-therapy counts of voxels surpassing the functional connectivity statistical significance threshold ( $z > 0.3$ ) show decreased variance following BCI therapy (Figure S4). No statistically significant correlations were observed between voxel count changes and motor recovery (Figure S5).

### 3.4. ROI-ROI and interhemispheric connectivity

Circular graph representations show median functional connectivity strengths pre-therapy for contra- and ipsilesional ROIs, based on  $z$ -scores of Pearson correlations between paired ROI nodes (Figure 5(a)). Strong connectivity strengths ( $z > 0.6$ ) characterized links between cortical motor ROI with connections located entirely contralesional or ipsilesional and

most interhemispheric links (Figure 5(a)). Relatively weaker connectivity strengths ( $z < 0.5$ ) occurred between interhemispheric CBL and motor ROIs (e.g. cSMA to iPMA or iM1; cM1 to iM1 or iPMA). Generally, many nodes showed connectivity above the threshold to other motor ROIs, an expected feature of the motor network. All suprathreshold connectivity changes in BCI patients were negative from pre- to post-therapy timepoints, regardless of whether paired ROIs were contralesional, ipsilesional, or interhemispheric. (Figure 5(b)). Not shown are median connectivity changes of  $|z| < 0.1$ .

Functional connectivity strength in BCI patients was significantly lower post-therapy compared to pre-therapy. Normalized distributions of functional connectivity strengths pre- and post-therapy are shown in Figure 6. The analysis included all ROI pairs regardless of a threshold of  $z > 0.3$  for results shown in Figure 5. A Wilcoxon signed-rank test found statistically significant decreases from pre- to post-therapy timepoints across all motor ROIs and patients ( $p = 1 \times 10^{-6}$ ), all interhemispheric motor ROI ( $p = 0.006$ ), all ipsilesional intrahemispheric ROI pairs (Figure 6(d),  $p = 0.003$ ), but not any contralesional intrahemispheric ROI pairs (Figure 6(c),  $p = 0.071$ ). These results showed

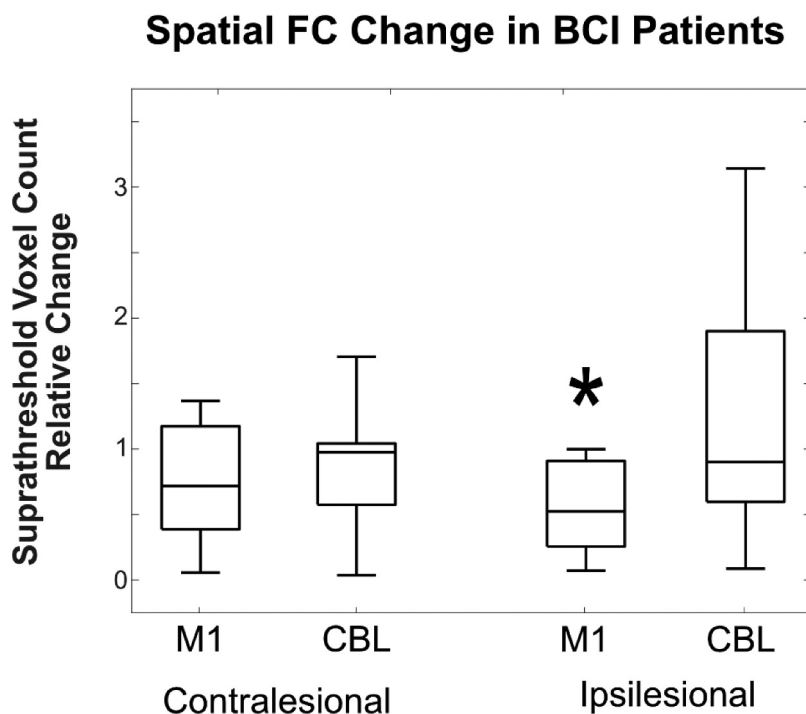


**Figure 4.** Normalized voxel count changes in select ROIs. Difference relative to baseline for the number of voxels with statistically significant functional connectivity ( $z > 0.3$ ) to contralesional and ipsilesional primary motor cortex (M1) and cerebellum (CBL) in chronic stroke patients pre- and post-therapy. Box-and-whisker plots indicate median values. Value of 1 indicates no change. The ipsilesional M1 region showed a statistically significant reduction in number of suprathreshold voxels compared to the pre-therapy timepoint with a Wilcoxon signed-rank test ( $p = 0.0156$ ).

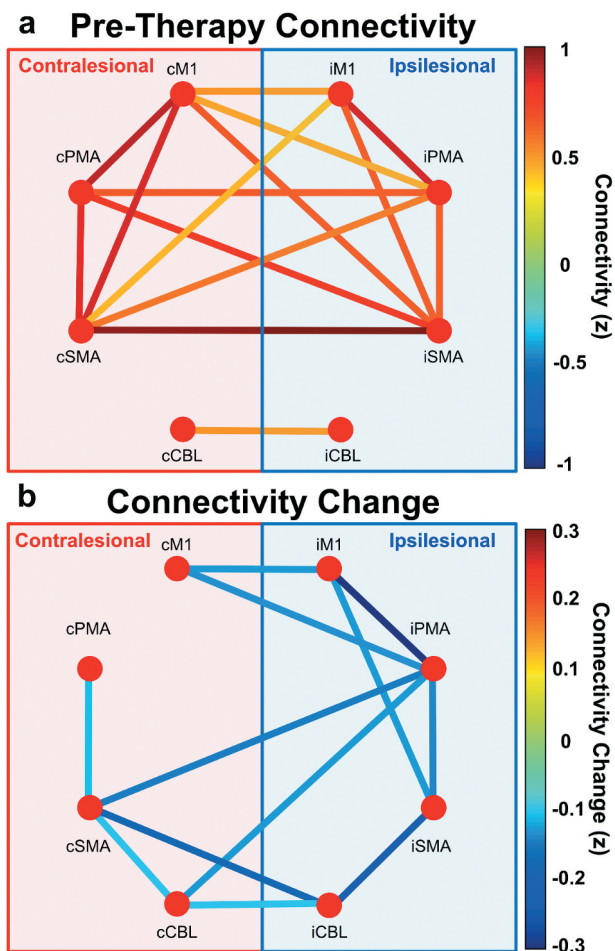


**Figure 5.** Functional connectivity changes in motor regions. (a) Median pre-therapy functional connectivity between motor ROI pairs in BCI patients. Primary motor, premotor, supplementary motor, and cerebellar ROIs used. Each node marks an ROI with a prefix specifying laterality (e.g. cSMA is contralateral supplementary motor area). Nodes in red and blue background areas are contralateral and ipsilateral ROIs, respectively. Line color indicates connectivity strength. Threshold of  $z = 0.3$  applied to connectivity graph. (b) Median change in connectivity from pre-therapy to post-therapy timepoints (post – pre) in BCI patients. Threshold of  $z = 0.1$  applied to connectivity graph.

contralateral BCI therapy significantly decreased motor network connectivity strength, regardless of hemisphere in relation to stroke location.

A key issue was whether motor recovery corresponded with decreases in motor connectivity. A nonparametric rank correlation analysis sorted patients by change in FC strength and extent of motor recovery. The analysis found that larger decreases in motor FC strength correlated with greater motor recovery (Figure 7(a)  $r = 0.77$ ,  $p = 0.033$ ). These significant findings indicated motor recovery through contralateral BCI therapy resulted in decreased overall motor intra-network functional connectivity. No other ROI sets showed connectivity changes correlated with recovery (Figure 7(b–d)).

## 4. Discussion

Upper extremity motor function improved in a chronic stroke population following 12 weeks of training with a noninvasive, contralaterally controlled brain–computer interface. Decreases in functional connectivity strength and topography in motor cortex ROIs were concurrent with upper limb motor improvements. Reductions in topographic connectivity to ipsilateral primary motor cortex correlated with recovery. Motor recovery levels were also significantly correlated with a reduction in functional connectivity strength. These findings suggest that contralateral BCI-induced motor function improvement in chronic stroke patients may be partially driven by widespread decreases in motor network functional connectivity.

Of particular importance was finding contralateral BCI therapy effectively enabled recovery for chronic hemiparesis. Chronic hemiparetic stroke patients usually experience poor motor recovery after 3 months post-stroke [5–9]. Studied patients were at a median of 62 months post-stroke. Nevertheless, 7 out of 8 patients made clinically significant improvements in upper limb motor function following contralateral BCI therapy. Ipsilateral BCI therapy for both acute and chronic hemiparesis has been previously implemented in a variety of configurations [12]. Robotic orthoses, electrical stimulation, and visual imagery feedback have all been used successfully in combination with ipsilateral BCI systems across several studies [12,13,16,52–55]. The current contralaterally driven BCI therapy method and intervention protocol replicated BCI-mediated recovery reported previously, thus confirming motor recovery with contralateral BCI therapy [17]. Critically, patients achieved motor improvement using BCI in a home therapy setting, with patients or their caretakers operating the BCI system. Others have recently noted the practical challenges of implementing BCI therapy in a clinical setting and suggested home-based therapy as a potential solution [54,56]. The current BCI approach advantageously expanded a therapy method previously confined to in-person clinical settings.

Acquisition of noninvasive functional neuroimaging concurrent with BCI therapy additionally revealed unexpected motor network changes during rehabilitation. Decreases in motor network functional connectivity strength suggest different network dynamics occur during recovery in chronic stroke compared to (sub)acute stroke. Typically, acutely injured networks characteristically showed increased intra- and decreased interhemispheric resting-state FC strength [24,25,30,33–35]. Task-based BOLD



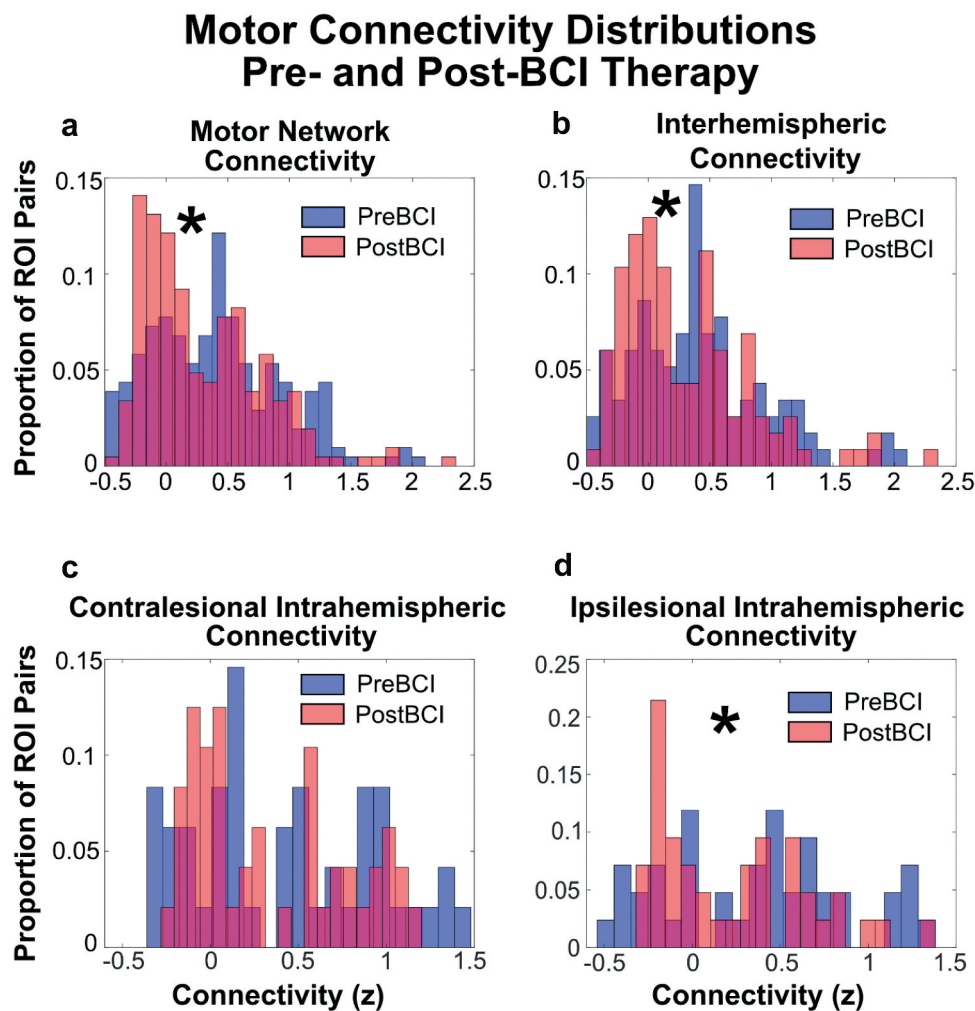


**Figure 6.** Motor connectivity decreases following BCI rehabilitation. Histograms constructed from motor ROI sets across all BCI patients at pre-therapy (blue) and post-therapy (red) timepoints. Overlapping histograms shown in purple. Histograms displays the normalized distribution of Z-transformed functional connectivity. ROI sets include all motor ROI pairs (a), interhemispheric ROI pairs (b), contralateral intra-hemispheric ROI pairs (c), and ipsilateral intra-hemispheric ROI pairs (d). Decreased post-therapy motor FC is statistically significant via Wilcoxon signed-rank test for full motor ROI set ( $p = 1 \times 10^{-6}$ ), interhemispheric ROI set ( $p = 0.006$ ), and ipsilateral intra-hemispheric ROI set ( $p = 0.003$ ). Contralateral intra-hemispheric connectivity decreased, but this change was not statistically significant ( $p = 0.071$ ).

activations during motor tasks also became lateralized toward the contralateral hemisphere [57]. With functional recovery in the subacute stage, brain function gradually reverted toward the pre-stroke state with increased interhemispheric connectivity and a return of ipsilateral cortical activation during a motor task [16,29,30,32,34,57,58]. Functional organization with more successful behavioral recovery resembled that of a healthy brain [29,30,32,58]. In contrast, contralaterally driven BCI therapy resulted in broadly decreased motor network intra- and interhemispheric connectivity strength. The findings also were not an epiphenomenon given a significant correlation between connectivity change and motor recovery.

Contralaterally driven BCI rehabilitation in chronic stroke may operate by affecting inhibitory circuit activity through experience-dependent plasticity. Mouse models of stroke recovery have indicated that experience-dependent plasticity may be important for stroke recovery. Studies in whisker barrel cortex suggest a possible model in which loss of incoming sensory input (e.g. removal of a whisker) resulted in robust alteration in the activity, connectivity, and structure of neural circuits [59]. Loss of input to a deprived barrel column precipitated a loss of inhibitory firing in that column. Unmasked horizontal excitatory connections possibly provoked expanded adjacent receptive fields serviced from neighboring columns linked to intact whiskers. These changes

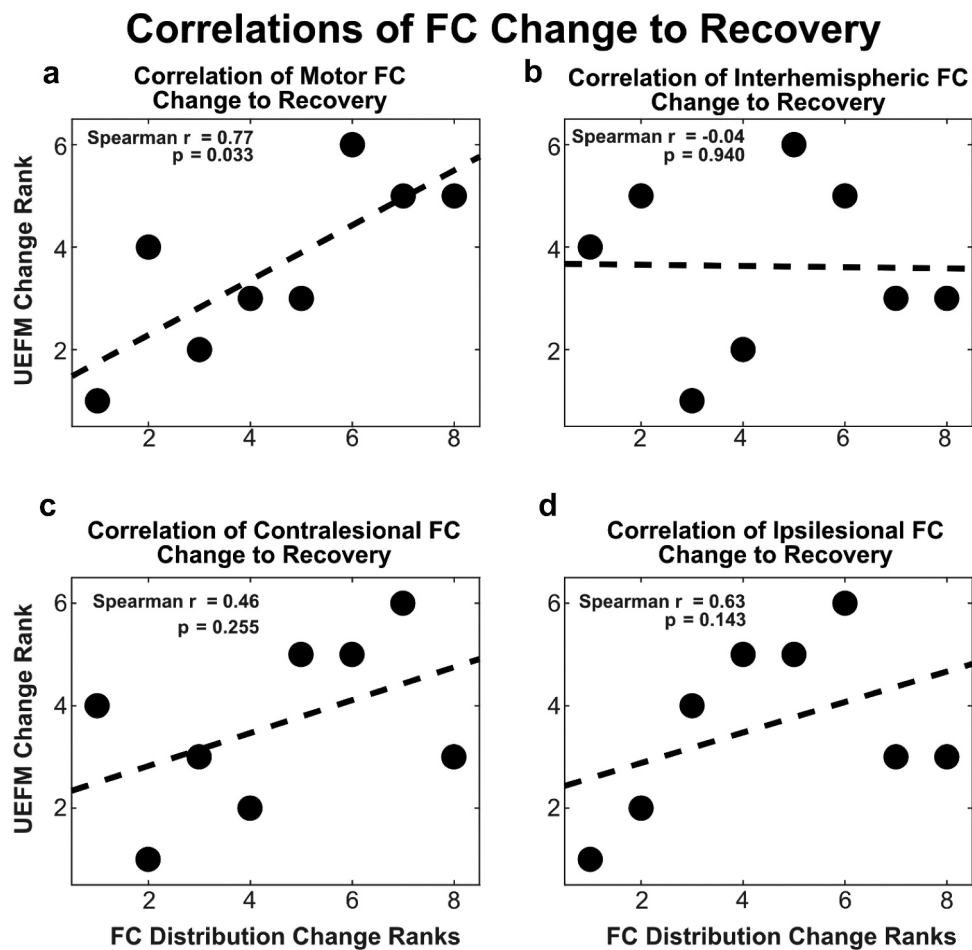


**Figure 7.** Correlation between connectivity change and BCI motor recovery. Spearman correlations between motor ROI connectivity change and motor recovery. Data represented in ranked form. The dotted line represents a least-squares regression fit onto the ranked data. Connectivity change in four ROI sets measured as shown in Figure 5. The correlation between connectivity change in all motor ROIs and motor recovery was statistically significant.

might be a consequent pathologic expansion of local connectivity [60]. Similar changes in cortical topographical maps arose from peripheral loss in nonhuman primates [61,62]. A possible mechanism affecting these network changes might be injury-induced downregulation of inhibitory circuits [62–64], allowing increased neural activity via *preexisting* thalamocortical and intracortical connectivity as opposed to *de novo* sprouting [65–67]. Similarly, provoked increases in intracortical connectivity might occur following stroke-mediated white matter transections in human cortex [68]. Consequently, chronic loss of motor output from stroke might pathologically diminish inhibitory activity, resulting in a net increase in maladaptive connectivity of the remaining motor network. This connectivity increase probably does not represent a compensatory mechanism, but rather a long-term pathologic end point of an injury. Thus, a consistent engagement of thalamocortical inhibitory motor rhythms with BCI usage may reverse this chronic

state of maladaptive, decreased inhibitory activity [18]. A consequence of the reversal could be the observed reduced motor functional connectivity, which may result from restored inhibitory activity. Further, enhanced inhibition might lead to increased functional specialization within the motor network, consistent with current findings of reduced nodal connectivity and diminished topographic distributions of connectivity (most notably in ipsilesional M1).

Ipsilesional primary motor cortex in BCI patients was the only ROI that showed a statistically significant change in suprathreshold voxels. Previous studies into motor network connectivity following acute stroke typically reported positive associations between ipsilesional M1 connectivity or activity and motor recovery – this does not match the presented findings [16,24,32,57]. While we observed no correlations between the degree of motor recovery and the change in ipsilesional M1 connectivity extent, there was an observed increase in a patient population achieving clinically significant recovery. The discrepancy may be due



to the specific design of the BCI device used for therapy. By promoting contralesional activity during therapy, activity-dependent plasticity may have altered functionally relevant ipsilesional activity. Extensive contralesional BCI use potentially resulted in reduced ipsilesional M1 connectivity specifically, in addition to the general decrease in motor network connectivity.

The current findings of BCI effects on motor recovery and decreased motor network connectivity indicate the importance of further optimization of BCI-mediated therapies. Previously, Bundy et al. demonstrated functional recovery correlated with patient accuracies of BCI control [17]. Thus, enhancing the personalization of BCI control to best facilitate patients' ability to control BCI therapy devices may be important for effective therapy [69]. The described methods used for BCI control in this study were relatively simple. The BCI system was controlled by the signal from a single electrode and a 1-Hz wide EEG frequency band associated with motor imagery. More elaborate control algorithms reliant on different EEG features may enhance rehabilitative effects. Further, other methods of feedback could include functional electric stimulation or virtual representations of a paretic hand moving [12,13,52,70–73]. In particular, the current feedback was only through proprioceptive sensation from moving the hand. Abundant evidence showed robotic manipulation of an affected limb has provided substantive benefit [12,13,52,70–72]. Designing an optimal feedback regimen to best affect identified motor network changes will require further research, possibly piloted initially in an animal model.

#### 4.1. Limitations

We executed a small, non-randomized, prospective study, which constrained the impact of these findings. The small sample size also constrained statistical testing to less powerful non-parametric tests, which may unreliably detect results from small effect sizes. Two BCI patients had multiple-stroke lesions, which may have further affected motor connectivity. However, we assumed these patients achieved full recovery from non-motor deficits due to our strict inclusion and exclusion criteria. Despite additional stroke effects in these cases, seven of eight patients showed clinically significant upper motor recovery after BCI therapy, which coincided with decreased in motor network connectivity.

#### 5. Conclusion

Chronic stroke patients used a contralesionally controlled BCI system to achieve clinically significant upper motor recovery. Motor recovery was coincident

with decreases in resting-state functional connectivity among motor ROIs. These findings are notably different from those in the subacute stage of stroke. Future studies need to explore the influence of BCI as a therapy for strokes affecting motor behavior.

#### Acknowledgments

The authors thank the study participants for their time and effort, and thank Kristina Zinn, Xin Hong, and Catherine Lang for providing the physical therapy data they worked to acquire.

#### Disclosure statement

Dr. Leuthardt owns stock in Neuroolutions, Inner Cosmos, and Sora Neuroscience. Washington University owns stock in Neuroolutions. Other authors report no conflicts. The funders had no role in study design, data collection and analysis, decision to publish, or preparation of the manuscript.

#### Funding

This work was supported by NIH R21NS102696 (Leuthardt and Carter) and NIH P41-EB018783.

#### References

- [1] Virani SS, Alonso A, Benjamin EJ, et al. Heart disease and stroke statistics—2020 update: a report from the American Heart Association. *Circulation*. 2020;141:E139–E596.
- [2] Lawrence ES, Coshall C, Dundas R, et al. Estimates of the prevalence of acute stroke impairments and disability in a multiethnic population. *Stroke*. 2001;32(6):1279–1284.
- [3] Sunderland A, Tinson D, Bradley L, et al. Arm function after stroke. An evaluation of grip strength as a measure of recovery and a prognostic indicator. *J Neurol Neurosurg Psychiatry*. 1989;52(11):1267–1272.
- [4] Wade DT, Langton-Hewer R, Wood VA, et al. The hemiplegic arm after stroke: measurement and recovery. *J Neurol Neurosurg Psychiatry*. 1983;46(6):521–524.
- [5] Duncan PW, Goldstein LB, Matchar D, et al. Measurement of motor recovery after stroke. *Stroke*. 1992;23(8):1084–1089.
- [6] Jorgensen HS, Nakayama H, Raaschou HO, et al. Outcome and time course of recovery in stroke. Part II: time course of recovery. The Copenhagen stroke study. *Arch Phys Med Rehab*. 1995;76(5):406–412.
- [7] Lloyd-Jones D, Adams R, Carnethon M, et al. Heart disease and stroke statistics - 2009 update. A report from the American heart association statistics committee and stroke statistics subcommittee. *Circulation*. 2009;119(3):480–486.

- [8] Hatem SM, Saussez G, Della Faille M, et al. Rehabilitation of motor function after stroke: a multiple systematic review focused on techniques to stimulate upper extremity recovery. *Front Hum Neurosci.* 2016;10:442.
- [9] Kwakkel G, Kollen B, Lindeman E. Understanding the pattern of functional recovery after stroke: facts and theories. *Restor Neurol Neurosci.* 2004;22(3-5):281-299.
- [10] Krakauer JW. Motor learning: its relevance to stroke recovery and neurorehabilitation. *Curr Opin Neurol.* 2006;19(1):84-90.
- [11] Langhorne P, Bernhardt J, Kwakkel G. Stroke rehabilitation. *Lancet.* 2011;377(9778):1693-1702.
- [12] Cervera MA, Soekadar SR, Ushiba J, et al. Brain-computer interfaces for post-stroke motor rehabilitation: a meta-analysis. *Ann Clin Transl Neurol.* 2018;5(5):651-663.
- [13] Biasucci A, Leeb R, Iturrate I, et al. Brain-actuated functional electrical stimulation elicits lasting arm motor recovery after stroke. *Nat Commun.* 2018;9(1):1-13.
- [14] Pichiorri F, Morone G, Petti M, et al. Brain-computer interface boosts motor imagery practice during stroke recovery. *Ann Neurol.* 2015;77(5):851-865.
- [15] Várkuti B, Guan C, Pan Y, et al. Resting state changes in functional connectivity correlate with movement recovery for BCI and robot-assisted upper-extremity training after stroke. *Neurorehabil Neural Repair.* 2013;27(1):53-62.
- [16] Ramos-Murguialday A, Broetz D, Rea M, et al. Brain-machine interface in chronic stroke rehabilitation: a controlled study. *Ann Neurol.* 2013;74(1):100-108.
- [17] Bundy DT, Souders L, Baranyai K, et al. Contralateral brain-computer interface control of a powered exoskeleton for motor recovery in chronic stroke survivors. *Stroke.* 2017;48(7):1908-1915.
- [18] Pfurtscheller G, Stancák A, Neuper C. Event-related synchronization (ERS) in the alpha band - An electrophysiological correlate of cortical idling: a review. *Int J Psychophysiol.* 1996;24(1-2):39-46.
- [19] Pfurtscheller G. Central beta rhythm during sensorimotor activities in man. *Electroencephalogr Clin Neurophysiol.* Published online 1981. DOI: 10.1016/0013-4694(81)90139-5.
- [20] Biswal B, Yetkin FZ, Haughton VM, et al. Functional connectivity in the motor cortex of resting human brain using echo-planar MRI. *Magn Reson Med.* 1995;34(4):537-541.
- [21] van den Heuvel MP, Hulshoff Pol HE. Exploring the brain network: a review on resting-state fMRI functional connectivity. *Eur Neuropsychopharmacol.* 2010;20(8):519-534.
- [22] Smitha KA, Akhil Raja K, Arun KM, et al. Resting state fMRI: a review on methods in resting state connectivity analysis and resting state networks. *Neuroradiol J.* 2017;30(4):305-317.
- [23] He BJ, Snyder AZ, Vincent JL, et al. Breakdown of functional connectivity in frontoparietal networks underlies behavioral deficits in spatial neglect. *Neuron.* 2007;53(6):905-918.
- [24] Carter AR, Astafiev SV, Lang CE, et al. Resting inter-hemispheric functional magnetic resonance imaging connectivity predicts performance after stroke. *Ann Neurol.* 2010;67(3):365-375.
- [25] Siegel JS, Ramsey LE, Snyder AZ, et al. Disruptions of network connectivity predict impairment in multiple behavioral domains after stroke. *Proc Natl Acad Sci U S A.* 2016;113(30):E4367-76.
- [26] Baldassarre A, Ramsey L, Hacker CL, et al. Large-scale changes in network interactions as a physiological signature of spatial neglect. *Brain.* 2014;137(12):3267-3283.
- [27] Ramsey LE, Siegel JS, Baldassarre A, et al. Normalization of network connectivity in hemispatial neglect recovery. *Ann Neurol.* 2016;80(1):127-141.
- [28] Gratton C, Nomura EM, Pérez F, et al. Focal brain lesions to critical locations cause widespread disruption of the modular organization of the brain. *J Cogn Neurosci.* 2012;24(6):1275-1285.
- [29] Siegel JS, Seitzman BA, Ramsey LE, et al. Re-emergence of modular brain networks in stroke recovery. *Cortex.* 2018;101:44-59.
- [30] Fan Y, Wu C, Liu H, et al. Neuroplastic changes in resting-state functional connectivity after stroke rehabilitation. *Front Hum Neurosci.* 2015;9(OCT):546.
- [31] Park C, Chang WH, Ohn SH, et al. Longitudinal changes of resting-state functional connectivity during motor recovery after stroke. *Stroke.* 2011;42(5):1357-1362.
- [32] Golestani AM, Tymchuk S, Demchuk A, et al. Longitudinal evaluation of resting-state fMRI after acute stroke with hemiparesis. *Neurorehabil Neural Repair.* 2013;27(2):153-163.
- [33] Lin LY, Ramsey L, Metcalf NV, et al. Stronger prediction of motor recovery and outcome post-stroke by cortico-spinal tract integrity than functional connectivity. *Boltze J, ed. PLoS One.* 2018;13(8):e0202504.
- [34] Baldassarre A, Ramsey LE, Siegel JS, et al. Brain connectivity and neurological disorders after stroke. *Curr Opin Neurol.* 2016;29(6):706-713.
- [35] Siegel JS, Mitra A, Laumann TO, et al. Data quality influences observed links between functional connectivity and behavior. *Cereb Cortex.* 2017;27(9):4492-4502.
- [36] Rossiter HE, Boudrias M-H, Ward NS. Do movement-related beta oscillations change after stroke? *J Neurophysiol.* 2014;112(9):2053-2058.
- [37] Westlake KP, Hinkley LB, Bucci M, et al. Resting state  $\alpha$ -band functional connectivity and recovery after stroke. *Exp Neurol.* 2012;237(1):160-169.
- [38] Sanford J, Moreland J, Swanson LR, et al. Reliability of the Fugl-Meyer assessment for testing motor performance in patients following stroke. *Phys Ther.* 1993;73(7):447-454.
- [39] Sullivan KJ, Tilson JK, Cen SY, et al. Fugl-Meyer assessment of sensorimotor function after stroke: standardized training procedure for clinical practice and clinical trials. *Stroke.* 2011;42(2):427-432.
- [40] Gladstone DJ, Danells CJ, Black SE. The Fugl-Meyer assessment of motor recovery after stroke: a critical review of its measurement properties. *Neurorehabil Neural Repair.* 2002;16(3):232-240.

- [41] Collin C, Wade D. Assessing motor impairment after stroke: a pilot reliability study. *J Neurol Neurosurg Psychiatry*. 1990;53(7):576.
- [42] Kopp B, Kunkel A, Flor H, et al. The Arm Motor Ability Test: reliability, validity, and sensitivity to change of an instrument for assessing disabilities in activities of daily living. *Arch Phys Med Rehabil*. 1997;78(6):615–620.
- [43] Bohannon RW, Smith MB. Interrater reliability of a modified Ashworth scale of muscle spasticity. *Phys Ther*. 1987;67(2):206–207.
- [44] Power JD, Mitra A, Laumann TO, et al. Methods to detect, characterize, and remove motion artifact in resting state fMRI. *Neuroimage*. 2014;84:320–341.
- [45] Fox MD, Zhang D, Snyder AZ, et al. The global signal and observed anticorrelated resting state brain networks. *J Neurophysiol*. 2009;101(6):3270–3283.
- [46] Power JD, Plitt M, Laumann TO, et al. Sources and implications of whole-brain fMRI signals in humans. *Neuroimage*. 2017;146:609–625.
- [47] Yarkoni T, Poldrack RA, Nichols TE, et al. Large-scale automated synthesis of human functional neuroimaging data. *Nat Methods*. 2011;8(8):665–670.
- [48] Seitzman BA, Gratton C, Marek S, et al. A set of functionally-defined brain regions with improved representation of the subcortex and cerebellum. *Neuroimage*. 2020;206:116290.
- [49] Hagberg AA, Swart PJ, Schult DA. Exploring network structure, dynamics, and function using networkx. *Proc 7th Python Sci Conf (SciPy 2008)*. Published online August 2008.:11–15.
- [50] Page SJ, Fulk GD, Boyne P. Clinically important differences for the upper-extremity Fugl-Meyer scale in people with minimal to moderate impairment due to chronic stroke. *Phys Ther*. 2012;92(6):791–798.
- [51] Bundy DT, Szrama N, Pahwa M, et al. Unilateral, Three-dimensional Arm Movement Kinematics are Encoded in Ipsilateral Human Cortex. *J Neurosci*. Published online October 8, 2018:0015–0018. DOI:10.1523/JNEUROSCI.0015-18.2018.
- [52] Ono T, Shindo K, Kawashima K, et al. Brain-computer interface with somatosensory feedback improves functional recovery from severe hemiplegia due to chronic stroke. *Front Neuroeng*. 2014;7(July):19.
- [53] Mukaino M, Ono T, Shindo K, et al. Efficacy of brain-computer interface-driven neuromuscular electrical stimulation for chronic paresis after stroke. *J Rehabil Med*. 2014;46(4):378–382.
- [54] Coscia M, Wessel MJ, Chaudary U, et al. Neurotechnology-aided interventions for upper limb motor rehabilitation in severe chronic stroke. *Brain*. 2019;142(8):2182–2197.
- [55] Carvalho R, Dias N, Cerqueira JJ. Brain-machine interface of upper limb recovery in stroke patients rehabilitation: a systematic review. *Physiother Res Int*. 2019;24(2):e1764.
- [56] Simon C, Bolton DAE, Kennedy NC, et al. Challenges and opportunities for the future of brain-computer interface in neurorehabilitation. *Front Neurosci*. 2021;15:814.
- [57] Cramer SC, Nelles G, Benson RR, et al. A functional MRI study of subjects recovered from hemiparetic stroke. *Stroke*. 1997;28(12):2518–2527.
- [58] van Meer MPA, van der Marel K, Wang K, et al. Recovery of sensorimotor function after experimental stroke correlates with restoration of resting-state inter-hemispheric functional connectivity. *J Neurosci*. 2010;30(11):3964–3972.
- [59] Kraft AW, Bauer AQ, Culver JP, et al. Sensory deprivation after focal ischemia in mice accelerates brain remapping and improves functional recovery through Arc-dependent synaptic plasticity. *Sci Transl Med*. 2018;10(426):31.
- [60] Kathleen Kelly M, Carvell GE, Kodger JM, et al. Sensory loss by selected whisker removal produces immediate disinhibition in the somatosensory cortex of behaving rats. *J Neurosci*. 1999;19(20):9117–9125.
- [61] Manger PR, Woods TM, Jones EG. Plasticity of the somatosensory cortical map in macaque monkeys after chronic partial amputation of a digit. *Proc R Soc B Biol Sci*. 1996;263(1372):933–939.
- [62] Jones EG. Cortical and subcortical contributions to activity-dependent plasticity in primate somatosensory cortex. *Annu Rev Neurosci*. 2000;23:1–37.
- [63] Hendry SHC, Jones EG. Reduction in number of immunostained GABAergic neurones in deprived-eye dominance columns of monkey area 17. *Nature*. 1986;320(6064):750–753.
- [64] Hendry SHC, Fuchs J, DeBlas AL, et al. Distribution and plasticity of immunocytochemically localized GABAA receptors in adult monkey visual cortex. *J Neurosci*. 1990;10(7):2438–2450.
- [65] DeFelipe J, Conley M, Jones EG. Long-range focal collateralization of axons arising from corticocortical cells in monkey sensory-motor cortex. *J Neurosci*. 1986;6(12):3749–3766.
- [66] Rausell E, Bickford L, Manger PR, et al. Extensive divergence and convergence in the thalamocortical projection to monkey somatosensory cortex. *J Neurosci*. 1998;18(11):4216–4232.
- [67] Rausell E, Jones EG. Extent of intracortical arborization of thalamocortical axons as a determinant of representational plasticity in monkey somatic sensory cortex. *J Neurosci*. 1995;15(6):4270–4288.
- [68] Hawasli AH, Kim DH, Ledbetter NM, et al. Influence of white and gray matter connections on endogenous human cortical oscillations. *Front Hum Neurosci*. 2016;10:10.
- [69] Raffin E, Hummel FC. Restoring motor functions after stroke: multiple approaches and opportunities. *Neuroscientist*. 2018;24(4):400–416.
- [70] Soekadar SR, Birbaumer N, Slutzky MW, et al. Brain-machine interfaces in neurorehabilitation of stroke. *Neurobiol Dis*. 2015;83:172–179.
- [71] Young BM, Williams J, Prabhakaran V. BCI-FES: could a new rehabilitation device hold fresh promise for stroke patients? *Expert Rev Med Devices*. 2014;11(6):537–539.
- [72] Foong R, Tang N, Chew E, et al. Assessment of the efficacy of EEG-Based MI-BCI with visual feedback and EEG correlates of mental fatigue for upper-limb stroke rehabilitation. *IEEE Trans Biomed Eng*. 2020;67(3):786–795.
- [73] López-Larraz E, Sarasola-Sanz A, Irastorza-Landa N, et al. Brain-machine interfaces for rehabilitation in stroke: a review. *NeuroRehabilitation*. 2018;43(1):77–97.